Neural network modulation, dynamics, and plasticity

Christian G. Fink, Michal Zochowski*, Victoria Booth*
*both authors contributed equally to this work

***Abstract*—Brain networks are unique in the plasticity of their synaptic structure and in the firing properties of neurons. In large, biophysical neuronal network models, we investigated the interaction of these plastic network properties with overall network dynamics. We simulated modulation of individual neurons by acetylcholine (ACh), a key neurotransmitter whose levels change across waking and sleep states, in networks whose synaptic connections were allowed to evolve according to a spike timing-dependent plasticity rule. Results showed that Ach-induced changes in cellular properties led to different network activity patterns that resulted in either overall synaptic strengthening or weakening. These results suggest that the action of ACh on neuron firing could participate in hypothesized sleep-related synaptic renormalization in the brain.**

Keywords—spike timing-dependent plasticity; sleep; acetylcholine; neural network; synchrony

I. Introduction

The brain's ability to adapt to an ever-changing environment is largely due to the ability of neurons to modify their synaptic connections, a phenomenon known as synaptic plasticity [1]. Despite the many benefits of synaptic plasticity, there are also efficiency costs, since strengthening synapses requires additional space and energy [2]. One recent hypothesis suggests that awake brains experience an overall strengthening of synapses, and that sleep is a periodic interval of down-scaling (or "synaptic renormalization") required to conserve space and energy [3]. Sleep is therefore "the price we pay for plasticity." While many recent studies support this hypothesis [4], the biophysical mechanisms which might drive wake-dependent synaptic up-scaling and sleep-dependent down-scaling are currently unknown.

One promising possibility is that dramatic differences in the concentrations of neuromodulators in the waking versus sleeping brain may differentially support overall up-scaling or down-scaling of brain networks [5-8]. One particularly prominent neuromodulator is acetylcholine (ACh), which is present at high concentrations in cortex during waking but is virtually absent during non-rapid eye movement (NREM) sleep. ACh has recently been shown to dramatically affect the phase response curves (PRCs) of cortical pyramidal neurons [9-10], which could dramatically alter their synchronization properties and in turn affect overall network potentiation.

To investigate this possibility, we simulated large, biophysical neural networks within which synaptic strength was modified according to a spike-timing dependent plasticity (STDP) rule. The effects of modulation by ACh upon overall network connectivity strength were explored. We found that the presence of ACh led to overall network potentiation, while the absence of ACh led to relative depotentiation, consistent with the synaptic renormalization hypothesis. Furthermore, introducing a cluster sub-structure to network connectivity led to stable potentiation of a subset of network connections in the absence of ACh, even while the rest of the network experienced overall depotentiation.

This work was supported by NSF CMMI 1029388 (MZ), NSF PoLS 1058034 (MZ), and NSF DMS-1121361 (VB).

Christian G. Fink is with the Department of Physics and Neuroscience Program, Ohio Wesleyan University, Delaware, OH 43015 USA (email: cgfink@owu.edu).

Michal Zochowski is with the Department of Physics and Biophysics Program, University of Michigan, Ann Arbor, MI 48109 (e-mail: michalz@umich.edu)

Victoria Booth is with the Departments of Mathematics and Anesthesiology, University of Michigan, Ann Arbor, MI 48109 (phone: 734-763-4730; fax: 734-763-0937; e-mail: vbooth@umich.edu).

II. Methods

A. Cortical neuron model

To model the effects of ACh on cortical pyramidal neurons, we used the neuronal model proposed in [10]. This enabled simulated modulation of acetylcholine concentration by varying a single parameter g_{Ks}, which is the maximum conductance associated with a slow, low-threshold potassium current [11]. g_{Ks} was set to 1.5 mS/cm^2 to model low ACh concentration and to 0 mS/cm^2 to simulate high ACh concentration. To compensate for different frequency-current curves, the driving current was set to 1.30 μA/cm^2 for low ACh concentration and to 0.08 μA/cm^2 for high ACh concentration. All other parameters remained constant and took the following values: g_{Na}=24.0 mS/cm^2, g_{Kdr}=24.0 mS/cm^2, g_L=24.0 mS/cm^2, V_{Na}=55.0 mV, V_K=-90.0 mV, and V_L=-60.0 mV [12].

B. Network connectivity

Our simulated networks consisted of 800 excitatory neurons and 200 inhibitory neurons. Connectivity structure was established using the Watts-Strogatz architecture [13]: each neuron was initially connected to its 8 nearest neighbors in a one-dimensional ring, and then each connection was broken with probability p and re-wired to another randomly-selected neuron. Synaptic current from neuron j to neuron i was specified by $I^{syn}_{ij}=w_{ij}\exp[-(t-t_{jk})/\tau]\,(V_i-E_{syn})$, where w_{ij} is the synaptic coupling strength, t_{jk} is the time of the k^{th} spike of neuron j, τ=0.5 ms, and E_{syn} is equal to 0 mV for excitatory synapses and -75 mV for inhibitory synapses.

C. Spike-timing dependent plasticity

An STDP model was used to modify the synaptic coupling strength values, w_{ij}, according to the temporal characteristics of neuronal firing. For a directed excitatory connection from pre-synaptic neuron j to post-synaptic neuron i, the connection was strengthened if neuron i fired shortly after neuron j fired, and the connection was weakened under the opposite firing sequence. This rule was mathematically formalized according to the equation

$$\Delta w_{ij} = \begin{cases} A_+ e^{-|\Delta t|/\tau_+}, & \text{if} \quad \Delta t > 0 \\ -A_- e^{-|\Delta t|/\tau_-} & \text{if} \quad \Delta t < 0 \end{cases} \tag{1}$$

Δw_{ij} is the additive change in synaptic strength that occurs due to the spike pairing, and Δt is the spike time of neuron i minus the spike time of neuron j. τ_+ and τ_- were set to10 ms in all simulations, and each synaptic coupling strength w_{ij} was constrained to remain in the interval $[0, w_{max}]$, with $A_+ = A_- = w_{max}/10$.

D. Network potentiation

The synaptic coupling strengths w_{ij} continually changed throughout a simulation as pre-post spike pairings continually occurred. We quantified the overall level of network potentiation by performing a linear transformation of the mean of all coupling strength values,

$$\text{Network Potentiation} = 2\,(w_{avg}/w_{max}) - 1 \qquad (2)$$

The Network Potentiation is therefore a normalized measure constrained to the interval [-1, 1]. It can be calculated at any time within a simulation. We used this measure to characterize the effects of high and low ACh concentration upon the overall level of potentiation of each network.

E. Network synchrony

Phase-locking synchrony of neurons was quantified using the mean phase coherence (MPC) measure, σ [14]. This is a pairwise measure defined by the equations

$$\sigma_{i,j} = \left| \frac{1}{N} \sum_{k=1}^{N} e^{i\phi_{i,j}^{k}} \right|$$
$$\phi_{i,j}^{k} = 2\pi \left(\frac{t_{j,k} - t_{i,k}}{t_{i,k+1} - t_{i,k}} \right) \qquad (3)$$

Here $t_{j,k}$ is the time of the k^{th} spike of neuron j, $t_{i,k}$ is the time of the spike of neuron i that is largest while being less than $t_{j,k}$, $t_{i,k+1}$ is the time of the spike of neuron i that is smallest while being greater than or equal to $t_{j,k}$, and N is the number of spikes of neuron j. The overall mean phase coherence measure for an entire network is simply the mean of the pairwise values over all possible neuronal pairs, constrained to the interval [0, 1].

III. RESULTS

A. Effects of ACh upon network dynamics and network potentiation

Modulating the concentration of ACh dramatically affected both network dynamics and network potentiation, as shown in Fig. 1. Panels A and C show that high concentration of ACh led to highly *asynchronous* network activity, while low concentration of ACh led to highly *synchronous* network activity. This was a result of acetylcholine's effect upon a slow, adaptation-inducing potassium current, which switched the excitability of the neurons from being Type II for low ACh concentration to Type I for high ACh concentration [11, 15].

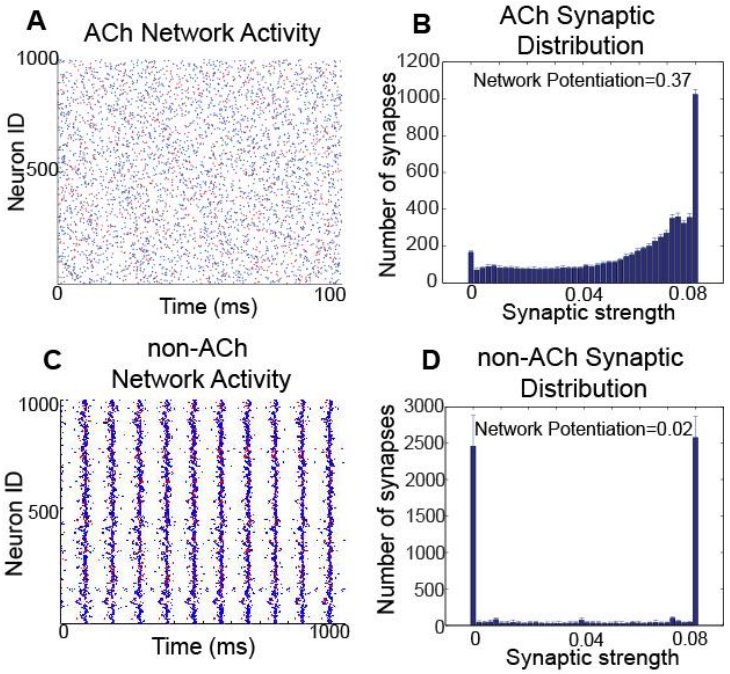

Figure 1: Effects of modulation of acetylcholine concentration upon network dynamics and network potentiation. (A) Raster plot of network activity for high ACh concentration, where each dot indicates the spike time of a particular neuron. Blue dots correspond to excitatory cells, while red dots correspond to inhibitory cells. (B) Equilibrium distribution of synaptic strength values for high ACh concentration. (C) Raster plot of network activity for low ACh concentration. (D) Equilibrium distribution of synaptic strength values for low ACh concentration. These results were obtained using a re-wiring probability of 0.60 and setting w_{max}=0.08 mS/cm^2. This figure is adapted from [12].

The difference in network synchrony dramatically influenced network potentiation, as shown in panels B and D. These plots show typical distributions of synaptic strength after sufficiently long simulation time to allow the distributions to equilibrate. The distribution resulting from high ACh concentration is clearly skewed toward the maximum possible synaptic strength, which results in much higher network potentiation than the low-ACh distribution, which is highly polarized between the maximum and minimum synaptic strengths.

The dramatic difference in network potentiation induced by varying ACh concentration was a direct result of the difference in network dynamics: the highly synchronous activity induced by low ACh concentration constrained all neurons to fire in a very short time window, resulting in approximately half of all synapses being strengthened and half being weakened within any one network burst. On the other hand, the neuronal activity induced by high ACh concentration was asynchronous but not random, so that pre-synaptic neurons were statistically more likely to fire right before their post-synaptic partners, resulting in the observed positive skew in the distribution of synaptic strength [12].

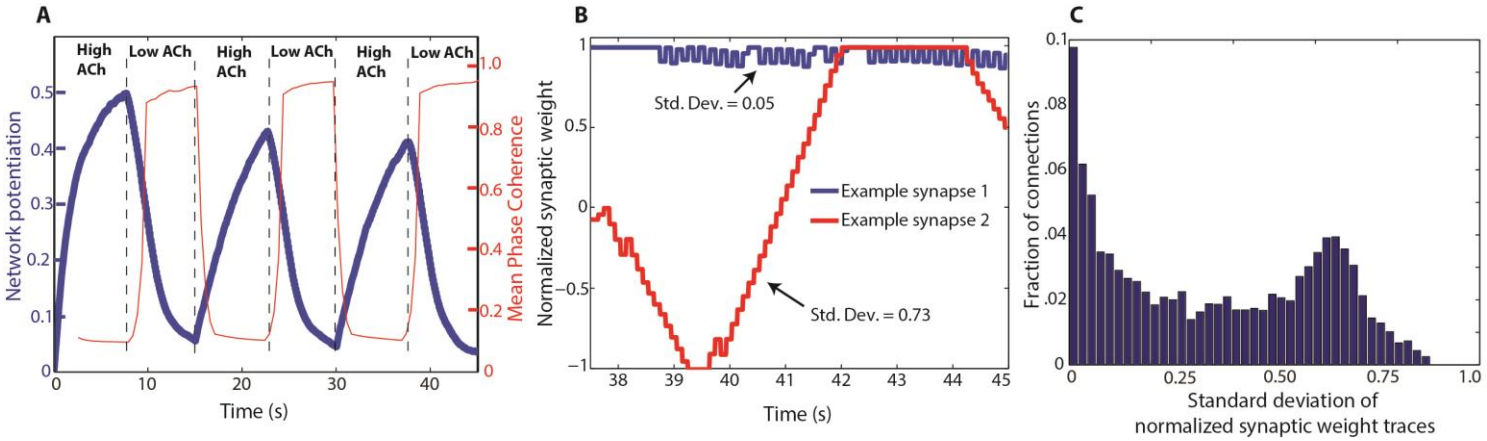

Figure 2: Effects of successive switching between high- and low-ACh concentration. (A) Network potentiation (blue line) and network synchrony as measured by mean phase coherence (red line) versus time as ACh concentration periodically switches. (B) Example traces of the normalized strengths of two synapses over time during the third low-ACh epoch. Note how the trace of the less stable synapse has a much higher standard deviation than that of the more stable synapse. (C) Histogram of the standard deviations of all synaptic strength traces from the third low-ACh epoch. Note the large proportion of synapses with large standard deviation.

B. Switching between high- and low-ACh states

Motivated by the fact that the cortex switches between high ACh concentration during waking and low ACh concentration during NREM sleep, we ran simulations in which the same network was successively switched between high and low ACh concentration. Fig. 2A shows that network potentiation rapidly increased when the network was switched to high ACh concentration, then rapidly decreased when switched to low ACh concentration. As before, increased network potentiation was associated with asynchronous network dynamics, while decreased network potentiation correlated with elevated network synchrony.

One question of interest was whether synapses tended to maintain the same strength during low-ACh states, since sleep-dependent memory consolidation is thought to stabilize synapses [16]. Fig. 2B shows example traces of the normalized synaptic strength (using Eq. 2) for two synapses during the third low-ACh epoch. The first synapse is relatively stable, while the second is not. We quantified the stability of each synapse in the network by calculating the standard deviation of each trace, with more stable synapses having lower standard deviation values. Fig. 2C shows a histogram of these values for all plastic synapses. While many synapses had low standard deviations, many also had values approaching that of the second trace in Fig. 2B, indicating the presence of a large number of unstable synapses.

C. Stabilizing effect of an embedded cluster

Fig. 3 shows the stabilizing effect of introducing an embedded cluster into the network. A cluster of 100 neurons and the remaining 900 neurons in the rest of the network were constructed as separate Watts-Strogatz small-world networks, each with a re-wiring probability of 0.60. Connections were then added from the cluster to the rest of the network and vice versa, with the connections originating in the cluster allowed to attain a higher maximum synaptic strength value, w_{max}, than the other connections in the network.

Fig. 3A shows that in total, all connections showed a cumulative increase in network potentiation when ACh concentration was high and a decrease in network potentiation when ACh concentration was low, as in Fig. 2A. However, the subset of connections that originated in the cluster and projected to the rest of the network showed very high network potentiation throughout the simulation, and actually increased in strength during epochs of low ACh concentration, during which the rest of the connections were collectively depotentiated. Connections originating in the rest of the network and projecting to the cluster showed the opposite trend. This effect was a result of the cluster synchronously driving the rest of the network during low-ACh epochs [12].

Furthermore, the connections originating within the cluster and projecting to the rest of the network were much more stable during low-ACh epochs than connections throughout the rest of the network. Fig. 3B shows how the distribution of standard deviation values for cluster-originating synapses during the third low-ACh epoch was highly skewed toward small values, while the analogous histogram for all other synapses shows a heavy tail (Fig. 3C).

IV. DISCUSSION

We have used a large-scale, biophysical neuronal network model to simulate the effects of modulation of ACh concentration upon network dynamics and network potentiation. We found that switching from high to low ACh concentration switched the network from asynchronous to synchronous activity, which was a result of ACh switching the excitability type of the model neurons. This dramatic change in network dynamics in turn led to overall depotentiation of the network through a spike-timing dependent plasticity rule. Successive switching between high and low ACh concentration led to perpetual alternation between network potentiation and depotentiation, a phenomenon that is consistent with sleep-dependent synaptic renormalization.

Introducing a cluster structure to network connectivity maintained this alternation between synaptic upscaling and downscaling, but in addition the subset of synapses originating within the cluster remained highly potentiated throughout ACh switching. This effect was robust not only at the network level, but was also stable at the level of individual synapses (see Figs. 3B and 3C), providing a simple paradigm for how

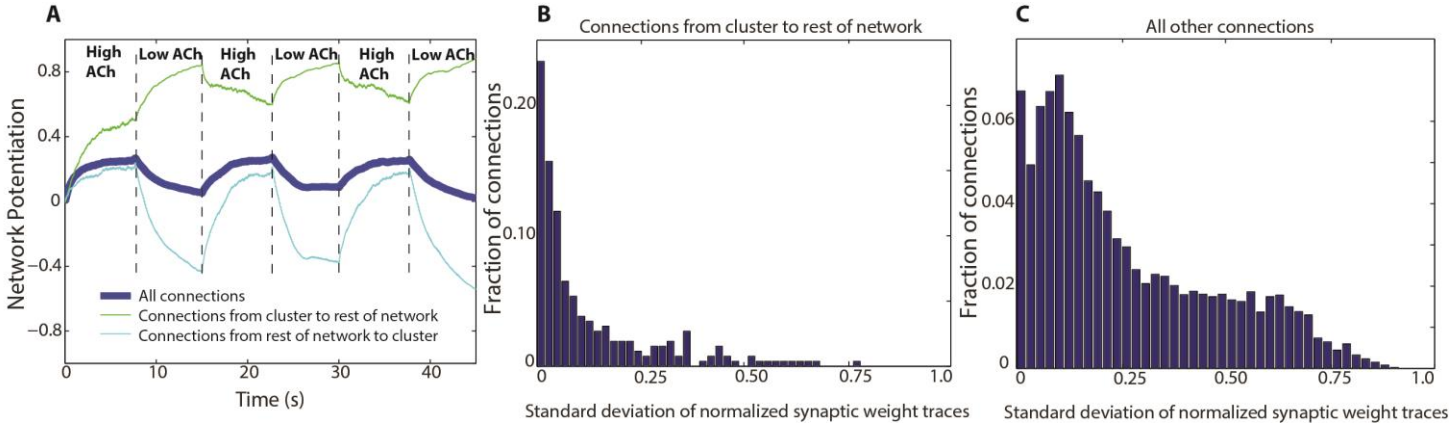

Figure 3: Network potentiation and synaptic stability for a network with an embedded cluster. (A) Network potentiation of various sets of synapses over time, as ACh is switched between high and low concentration. (B) Histogram of standard deviations of synaptic strength traces for connections originating in the cluster and projecting outside the cluster. (C) Histogram of standard deviations of synaptic strength traces for all connections in the network *except* those depicted in panel B. Note the heavy tail in C compared to B, indicating the greater stability of synapses originating within the cluster. B and C were constructed from data from the third low-ACh epoch.

overall sleep-dependent synaptic downscaling may occur while allowing for stable potentiation of a small subset of connections.

While our model suggests that acetylcholine may play an important role in synaptic renormalization, there are many other mechanisms which may contribute as well. The processing of sensory input may promote overall synaptic upscaling during waking states [3], while the highly synchronous thalamocortical activity which generates delta waves during NREM sleep could contribute to synaptic downscaling. Other studies have also suggested that neuromodulators in addition to acetylcholine, such as noradrenaline, may contribute to synaptic renormalization [17, 18]. Finally, while this study focused specifically upon spike-timing dependent plasticity, there are myriad other forms of plasticity whose effects should be explored. Further investigation is clearly needed in order to provide a biophysical basis for synaptic renormalization.

REFERENCES

[1] M.F. Bear and R.C. Malenka, "LTP and LTD: An embarrassment of riches," Neuron, vol. 44, pp. 5-21, September 2004.

[2] G. Tononi and C. Cirelli, "Sleep and synaptic homeostasis: a hypothesis," Brain Research Bulletin , vol. 62, pp. 143–150, 2003.

[3] G. Tononi and C. Cirelli, "Sleep function and synaptic homeostasis," Sleep Medicine Reviews, vol. 10, pp. 49-62, 2006.

[4] E. Hanlon, V. Vyazoyskiy, U. Faraguna, G. Tononi, and C. Cirelli, "Synaptic potentiation and sleep need: Clues from molecular and electrophysiological studies," Current Topics in Medicinal Chemistry, vol. 11, pp. 2472–2482, 2011.

[5] U. Olcese, S. Esser, and G. Tononi, "Sleep and synaptic renormalization: A computational study," Journal of Neurophysiology, vol. 104, pp. 3476–3493, 2010.

[6] G. Seol, J. Ziburkus, S. Huang, L. Song, I. Kim, et al., "Neuromodulators control the polarity of spike-timing-dependent synaptic plasticity," Neuron, vol. 55, pp. 919–929, 2007.

[7] S. Brocher, A. Artola, and W. Singer, "Antagonists and cholinergic and noradrenergic receptors facilitate synergistically the induction of long-term potentiation in slices of rat visual cortex," Brain Research, vol. 573, pp. 27–36, 1992.

[8] K. Stiefel, F. Tennigkeit, and W. Singer, "Synaptic plasticity in the absence of backpropagating spikes of layer II inputs to layer V pyramidal cells in rat visual cortex," European Journal of Neuroscience, vol. 21, pp. 2605–2610, 2005.

[9] K. Stiefel, B. Gutkin, and T. Sejnowski, "Cholinergic neuromodulation changes phase response curve shape and type in cortical pyramidal neurons," PLoS ONE, vol. 3, e3947, 2008.

[10] K. Stiefel, B. Gutkin, and T. Sejnowski, "The effects of cholinergic neuromodulation on neuronal phase-response curves of modeled cortical neurons," Journal of Computational Neuroscience, vol. 26, pp. 289–301, 2009.

[11] C.G. Fink, V. Booth, and M. Zochowski, "Cellularly-driven differences in network synchronization propensity are differentially modulated by firing frequency," PLoS Computational Biology, vol. 7, e1002062, 2011.

[12] C.G. Fink, G.G. Murphy, M. Zochowski, and V. Booth, "A dynamical role for acetylcholine in synaptic renormalization," PLoS Computational Biology, vol. 9, e1002939, 2013.

[13] D.J. Watts and S.H. Strogatz, "Collective dynamics of small-world networks," Nature, vol. 393, pp. 440-442, 1998.

[14] F. Mormann, K. Lehnertz, P. David, and E. Elger, "Mean phase coherence as a ameasure for phase synchronization and its application to the EEG of epilepsy patients," Physica D, vol. 144, pp. 358-369, 2000.

[15] B. Ermentrout, M. Pascal, and B. Gutkin, "The effects of spike frequency adaptation and negative feedback on the synchronization of neural oscillators," Neural Computation, vol. 13, pp. 1285-1310, 2001.

[16] S. Diekelmann and J. Born, "The memory function of sleep," Nature Reviews Neuroscience, vol. 11, pp. 114-126, 2010.

[17] U. Olcese, S. Esser, and G. Tononi, "Sleep and synaptic renormalization: A computational study," Journal of Neurophysiology, vol. 104, pp 3476-3493, 2010.

[18] G. Seol, J. Ziburkus, S. Huang, L. Song, and I. Kim, "Neuromodulators control the polarity of spike-timing-dependent synaptic plasticity," Neuron, vol. 55, pp. 919-929, 2007.